

Phase stability in the drifting subpulse pattern of PSR 0809 + 74

S. C. Unwin *Mullard Radio Astronomy Observatory, Cavendish Laboratory, Madingley Road, Cambridge CB3 0HE*

A. C. S. Readhead, P. N. Wilkinson and M. S. Ewing
California Institute of Technology, Pasadena, California 91125, USA

Received 1977 August 26

Summary. Observations of PSR 0809 + 74 have been made at 225 MHz to study the stability of its drifting subpulse pattern, and in particular the effect of pulse nulls on the phase of subpulse bands. It is found that a jump of phase occurs at each null. The magnitude of the jump implies that the subpulse bands cease drifting for the duration of the null. If allowance is made for these phase jumps, the periodicity of the subpulse bands varies in the long term by less than one part in 250. The relevance of these results for pulsar models is discussed.

1 Introduction

The pulsar emission mechanism is not well understood in spite of the large quantity of observational data now available. This is partly due to the difficulty of the theoretical problems involved, but also to the diversity of behaviour seen in different pulsars. In some cases the pulse position drifts systematically from pulse to pulse across a window defined by the mean pulse envelope (Drake & Craft 1968; Backer 1970; Cole 1970), and we believe, with Page (1973), that a detailed study of these objects may provide the key to understanding the phenomenon as a whole.

PSR 0809 + 74 exhibits the simplest behaviour of this type. All of the observed radiation occurs in drifting subpulses, and the variations in subpulse-band drift rate are comparatively small. We have therefore made extensive observations of PSR 0809 + 74 at 225 MHz to study the details of the drifting subpulse pattern.

2 The observations

The observations were made between 1975 September 18 and 22 at the Owens Valley Radio Observatory with the 40-m telescope, operating at 225 MHz with a circularly polarized feed. The pulsar was observed continuously during this period with an integration time and data sampling rate of 20 ms and 100 Hz, respectively. To minimize the effect of interstellar scattering we used the largest possible bandwidth compatible with the detection of adjacent

subpulse bands. The chosen value of 5.5 MHz resulted in a pulse dispersion smearing of 23 ms, i.e. about half the separation of successive subpulses (53 ms); it also reduced the interstellar scintillation considerably, and there were typically 1–2 hr between deep minima in the scintillation pattern, enabling us to monitor the subpulse bands continually for up to an hour at a time. The smearing of 23 ms was too large to permit an accurate determination of subpulse widths, but the mean pulse envelope is highly symmetric and has a width consistent with the value of 45 ms observed by Lyne, Smith & Graham (1971) at 240 MHz.

3 Analysis of the drifting subpulses

3.1 METHODS OF ANALYSIS

Fig. 1 shows a typical example of the drifting subpulse behaviour. Each row displays the intensity of the subpulse(s), in a single pulse, sampled at intervals of 10 ms across the pulse window. Successive rows show pulse windows separated by the basic pulse period, $P_1 = 1.2922$ s. As a first step in the analysis, all the data were displayed in this form. As is clearly seen, subpulses start at the trailing edge of the pulse window and move systematically forward (i.e. they occur earlier in successive pulses), thus giving rise to subpulse bands. The diagram shows

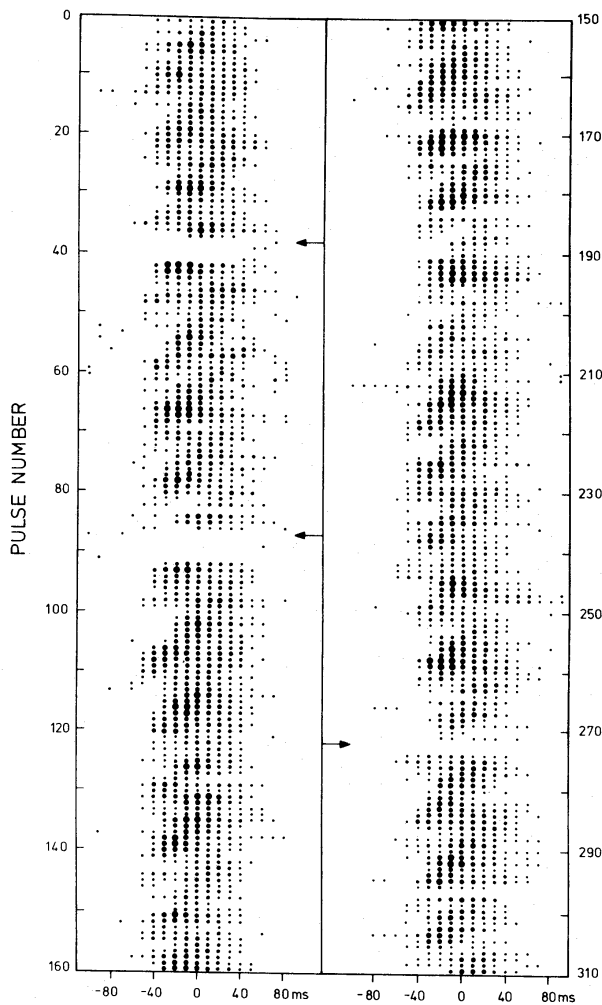


Figure 1. Typical longitude–time diagram of PSR 0809 + 74 at 225 MHz showing three nulls (arrowed). Observation of 1975 September 19, 23^h 12^m UT.

that, when the bands of subpulses are not interrupted by nulls, they repeat with remarkable regularity at intervals close to $11P_1$. Taking zero longitude as the centre of the window defined by the mean pulse envelope, we can conveniently define the phase, $\psi(N)$, of the N th subpulse band in units of P_1 :

$$\psi(N) = t(N)/P_1 - 11N \quad (1)$$

where $t(N)$ is the time at which the N th band crosses zero longitude.

To study the behaviour of $\psi(N)$ over long periods of time, subpulse-band diagrams like Fig. 1 could be used but a more objective approach is to cross-correlate the data with a matched filter, and thus achieve the maximum possible signal-to-noise ratio for the detection of subpulse bands. We constructed a matched filter by adding a large number of subpulse bands (Fig. 2). To allow for variations in the drift-rate of subpulse bands, D (measured in units of ms/P_1), the slope of the ideal band was varied. If the drift-rate, D , is constant with longitude then $D = P_2/P_3$, where P_2 is the separation between successive subpulses within a single pulse, and P_3 ($\approx 11P_1$) is the separation of adjacent subpulse bands (see e.g. Page 1973).

The three filters shown in Figs 2(a), (b) and (c) have drift-rates of 3.7, 4.3 and 4.9 ms/P_1 respectively. These were cross-correlated with the data, and the result normalized in the usual way to give the correlation coefficient. Since the filters increased the sensitivity for the detection of subpulse bands, it proved possible to follow these through sections of data in which the signal was too weak for the bands to be picked out easily by eye from the plots of subpulse bands (Fig. 1).

An example of the correlation observed in this way is shown in Fig. 3, illustrating the responses of the three filters to the subpulse bands, and to a null commencing at pulse number 79. The correlation coefficient drops at a null because incomplete bands are being correlated. Using this method, we can determine the phase of subpulse bands to within about 1 unit.

3.2 CHARACTERISTICS OF NULLS

When a null occurs, no radiation is observed from the pulsar, and as can be seen from Fig. 1, the time taken to turn off or on is $\lesssim P_1$. This affects both leading and trailing subpulses when these are present in a single pulse. We can therefore define for each null a quantity $L = \Delta t/P_1 - 1$,

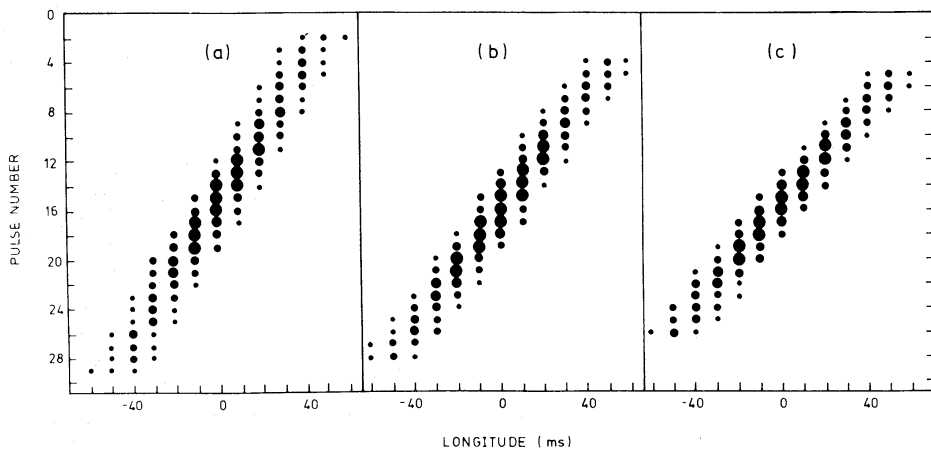


Figure 2. Correlation filters corresponding to three drift-rates used to measure subpulse-band phase. (a) 3.7 ms/P_1 , (b) 4.3 ms/P_1 , (c) 4.9 ms/P_1 .

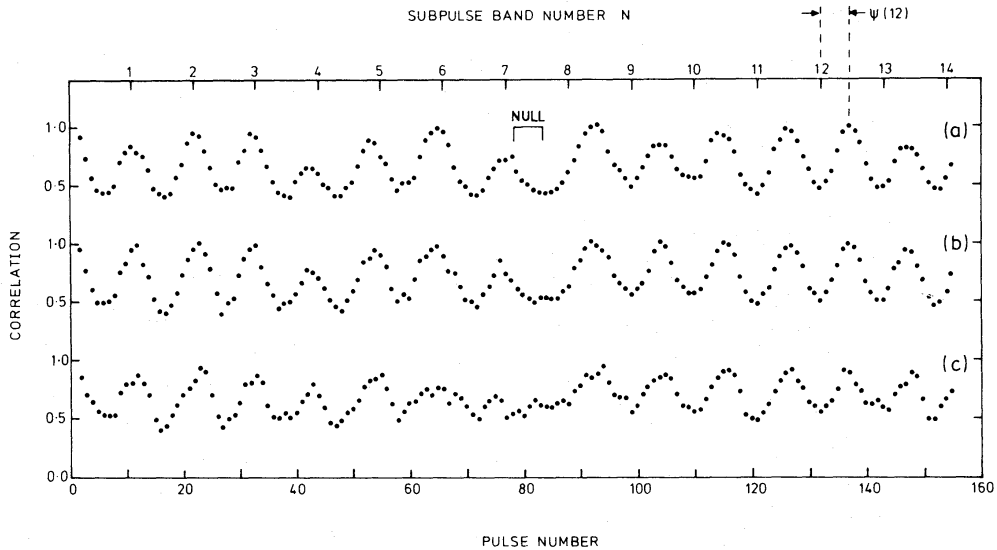


Figure 3. Cross-correlation diagram of PSR 0809 + 74 using three filters of Figs 2(a), (b) and (c) in Figs 3(a), (b) and (c) respectively. A null with $L = 5$ is indicated, starting at pulse number 79, and the measurement of ψ ($N = 12$) is illustrated. Observation of 1975 September 19, 23^h 25^m UT.

where Δt is the time for which no radiation is received. We have searched all the plots of subpulse bands (Fig. 1) of our data for nulls, and for each null we have measured the duration Δt , and hence L . Only those data were considered for which the signal-to-noise ratio is high. The ratio of signal strength during a null to that on either side of the null is found to be $< 1/25$ in a typical case.

A continuous distribution of null sizes L may exist, but only integral values can be observed from a given direction in space. The distribution of sizes for 45 nulls is shown in Fig. 4 and has a mean value $\bar{L} = 4.6$. It should be noted that nulls with $L = 1$ or 2 have been omitted in an attempt to ensure that all nulls considered are genuine. Nulls with $L \leq 2$ may in fact exist, but in practice these are masked by pulse to pulse intensity variations.

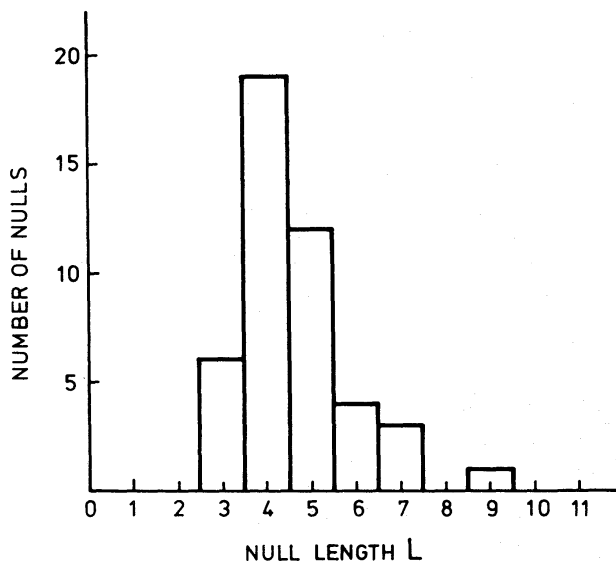


Figure 4. Distribution of null lengths (L) for 45 nulls.

Nulls occur at irregular intervals, and we have obtained a median interval between nulls in all our observations of approximately $30P_3 \approx 330P_1$. We have investigated the possibility that nulls may begin or end when subpulse bands reach a preferred longitude within the pulse window. By determining the longitude of subpulses of the last pulse before, and the first pulse after the null, in a total of 40 nulls, we conclude that no such preference exists. After a null, the first few pulses received often have greater intensity than the mean value before the null; occasionally this increase is more than 50 per cent.

3.3 PHASE BEHAVIOUR AT NULLS

The subpulse-band phase $\psi(N)$ was measured using the correlation plots (Fig. 3). In Fig. 3 we see that for all the subpulse bands preceding the null, the phase as defined by (1) is close to zero, i.e. $\psi(N) \sim 0$ for $N = 1$ to 7, whereas for those bands following the null the phase is approximately 5, i.e. $\psi(N) \sim 5$ for $N = 8$ to 13. From the subpulse-band plots we find that for this particular null $L = 5$. This apparent equality between L and $\Delta\psi(N)$ is investigated further below. It is important to emphasize here that the null duration (Δt or L) is determined, quite independently, from the plots of subpulse bands (Fig. 1), whereas the phase jumps are determined from the correlation plots (Fig. 3). Because the subpulse bands are disrupted immediately before and after nulls we used the subpulse-band plots to estimate the phase of the incomplete bands on either side of nulls, although it should be noted that this procedure is inherently less accurate than the use of correlation plots in the absence of nulls. In all cases this made only a very small difference, ~ 1 or 2, to the estimate of the subpulse-band phase.

Fig. 5(a) shows the subpulse phase plotted for successive bands for a section of data analysed in this way. Normally the phase $\psi(N)$ changes slowly with N , indicating that P_3 is always fairly close to $11P_1$; a value of P_3 above (below) $11P_1$ implies a steady increase (decrease) in phase. On short timescales the phase wander appears to be random, but on long timescales the phase stability, and hence that of P_3 , depends on the interpretation of the behaviour of subpulse bands around nulls, as will be discussed in Section 3.5.

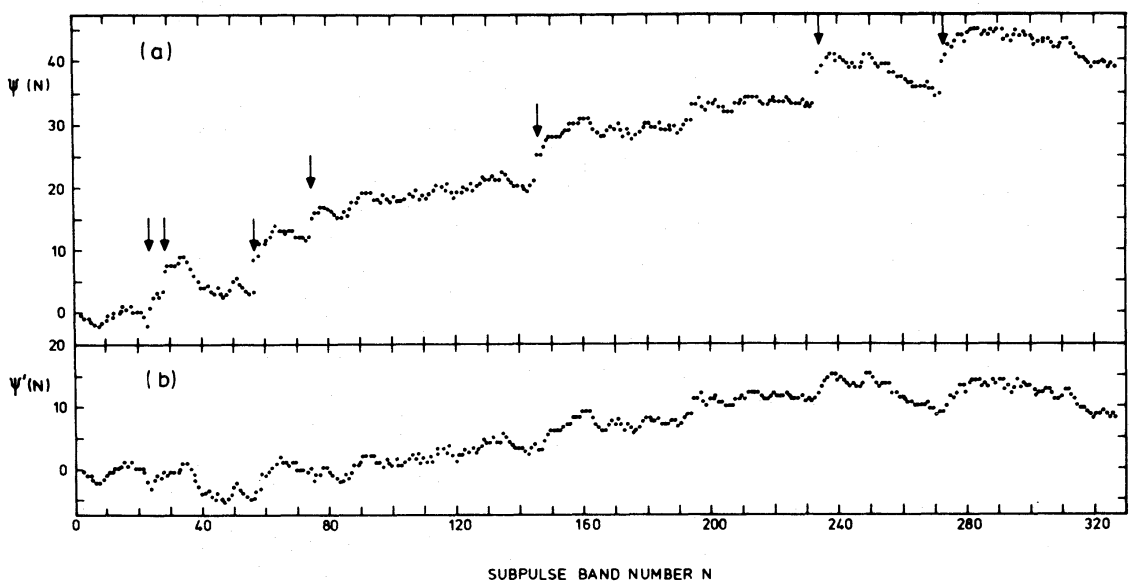


Figure 5. Subpulse-phase-time diagram, with null positions arrowed. (a) No allowance for phase jumps, (b) $\Delta\psi = LP_1$ for each null. Observation of 1975 September 21, 01^h 37^m UT.

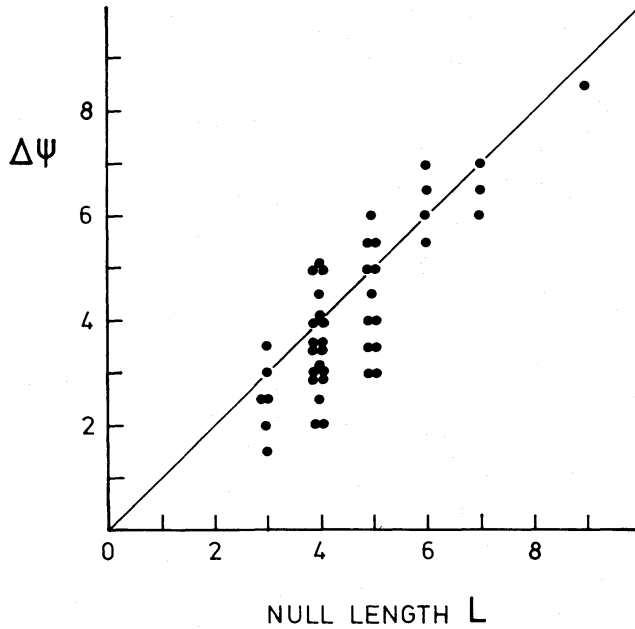


Figure 6. Relation between the phase jump $\Delta\psi$ and null length L for 45 nulls.

Fig. 5(a) illustrates that there is always a jump in phase at nulls, which are shown arrowed, and in Fig. 6 the lengths of the 45 nulls used in Fig. 4 are plotted against the phase jump $\Delta\psi$ determined from subpulse-band diagrams. This clearly shows that L and $\Delta\psi$ are nearly equal, and although it is possible that L and $\Delta\psi$ are exactly equal, this is difficult to demonstrate on individual nulls because of the short-term phase wander (Fig. 5).

The near equality of $\Delta\psi$ and L implies that the subpulse bands cease drifting for the duration of a null, and this leads to an alternative of subpulse phase which allows for the phase jumps at nulls:

$$\psi'(N) = t(N)/P_1 - 11N - \sum_{i=1}^j L_i \quad (2)$$

where L_i is the length of the i th null, and the summation is appropriate for values of N between the j th and $(j+1)$ th nulls, i.e. the phase of all bands after the i th null are retarded by L_i . The data of Fig. 5(a) have been replotted in Fig. 5(b) using (2) and it is evident that the phase discontinuities have disappeared, and $\psi'(N)$ varies smoothly throughout.

Page (1973) noted the jump in phase at nulls and, by subtracting a constant phase jump $\Delta\psi = 11$ for each null, he concluded that the phase returned to its slowly varying pre-null value after a few bands, corresponding to some form of relaxation after the absence of one whole subpulse band in the null. We have tested this conclusion by setting $L_i = 11$ for all i in (2) and find that the phase jumps (now in the opposite direction to that of Fig. 5(a)) remain, and the phase variations are not substantially reduced. Page's analysis was carried out on shorter stretches of data which made it more difficult to determine the local mean drift rate.

The validity of (2) can be illustrated in another way by showing, as in Fig. 7, the mean phase behaviour around a null, averaged over the 45 nulls in Figs 4 and 6, assuming different phase jumps $\Delta\psi$ at nulls. In Fig. 7(a), equation (1) was used for $\psi(N)$, so no allowance was made for phase jumps. In Fig. 7(b) we have subtracted a phase jump $\Delta\psi = 11P_1$ from each null as suggested by Page (1973) to obtain 7(b), and in Fig. 7(c) we put $\Delta\psi = L_i$

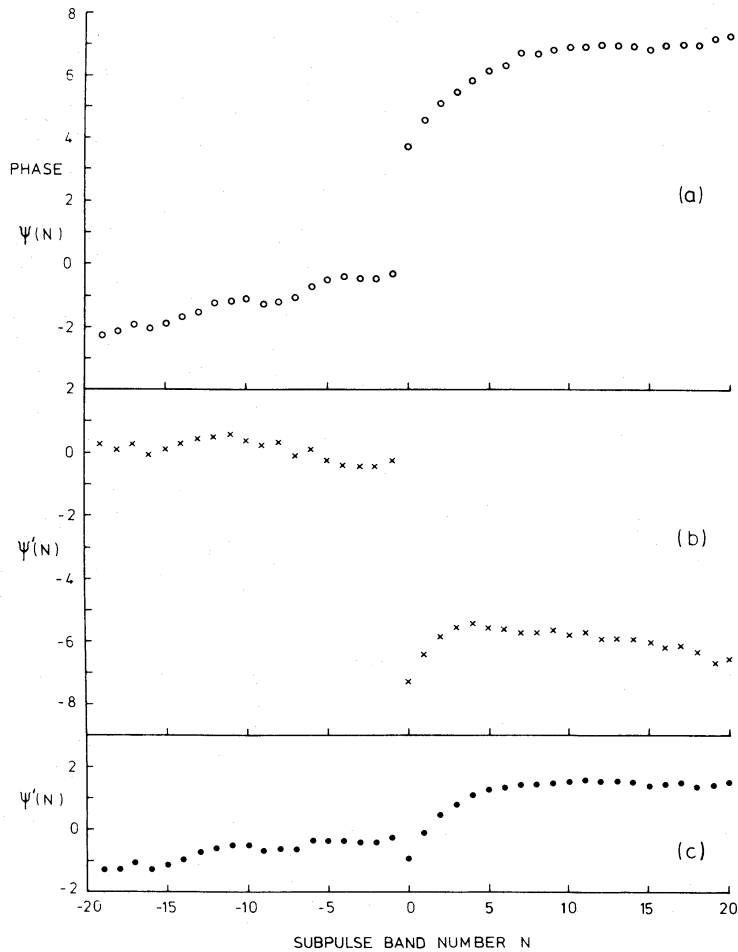


Figure 7. Mean phase behaviour around 45 nulls; (a) no allowance for phase jumps, (b) $\Delta\psi = 11P_1$ at each null, (c) $\Delta\psi = LP_1$ at each null.

according to (2) for each null, and clearly the result is to remove the phase jump almost completely. The shapes of the three curves (apart from the phase jump at $N = 0$) are not identical, since the occurrence of any two nulls separated by M bands modifies the mean phase for all $|N| > M$. The phase behaviour illustrated by Fig. 7 confirms the result expected from the relation in Fig. 6. The increase in phase for $N > 0$ corresponds to a reduction in drift rate D for 3–4 bands following a null. A similar effect was found by Page (1973), though here the maximum reduction in D is only ~ 10 per cent i.e. about one-third of that reported by Page. This change in the drift-rate shows that a phase jump is not the only effect of a null on the subpulse-band structure.

3.4 POWER SPECTRA OF SUBPULSE-BAND INTENSITY

As a further check on the interpretation of phase behaviour at nulls, we have performed a power-spectrum analysis on section of the data, using a method analogous to that of Taylor & Huguenin (1971). We assumed that the subpulse bands had a longitude drift-rate of $4.3 \text{ ms}/P_1$ and made use of the filter in Fig. 2(b); in fact, the spectra are not very sensitive to the assumed drift-rate. Samples of length 1024 pulses were used, and the filter removed components above a frequency $\sim 1/(11P_1)$. Fig. 8(a) shows the power spectrum obtained directly from a section of the data containing four nulls, making no allowance for any phase jumps.

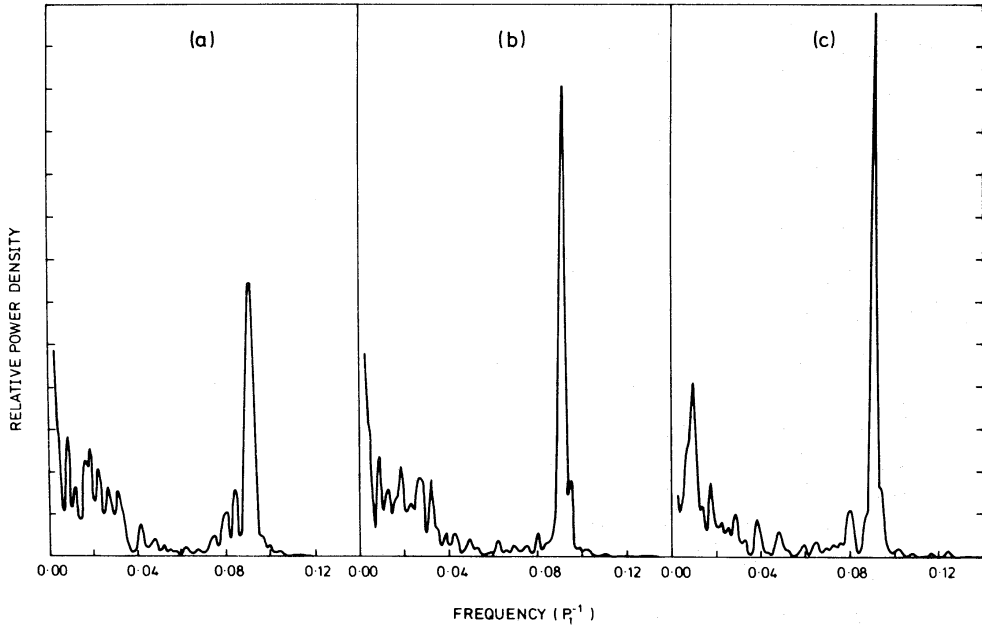


Figure 8. Power spectra of subpulse bands, with effective frequency resolution $0.002/P_1$: (a) observation of 1975 September 19, $23^{\text{h}} 08^{\text{m}}$ UT, (b) as (a) but with $\Delta\psi = LP_1$ for each of the four nulls in the record, (c) observation of 1975 September 20, $20^{\text{h}} 47^{\text{m}}$ UT.

In (b) the same data were used, but with the phase modified according to (2) by subtracting $\Delta t = LP_1$ from the phase for data following each null. The peak at a frequency $\sim 1/(11P_1)$ has narrowed considerably and increased in intensity, thus demonstrating the enhanced phase coherence; we have found this to be characteristic of all sections of data containing nulls. In Figs 8(a) and (b) the spectral features have Q values of 24 and 40 respectively. For comparison Fig. 8(c) shows, on a reduced intensity scale, the spectrum of a sample in which the phase was particularly stable, and for which no nulls were recorded. The peak at $1/(11P_1)$ has $Q = 80$, but much smaller values were found in general, since the phase stability over different lengths of data varied greatly.

A notable feature of Fig. 8 is the lack of peaks corresponding to integral multiples of the periodicity $11P_1$; with the resolution available in our spectra we have seen no significant peaks down to frequencies $\sim 1/(6 \times 11P_1)$. Autocorrelation analysis of the data out to lags of $\sim 45 \times 11P_1$ shows, likewise, no significantly higher correlation at any multiple of $11P_1$ after the first. Thus we have no evidence of any pattern recurring periodically on larger time scales than the basic subpulse pattern (P_3).

3.5 STABILITY OF P_3

The power-spectrum analysis of section 3.4 provides a method of determining the stability of P_3 by measuring the width of the spectrum obtained. An equivalent method is to measure P_3 and its stability from subpulse-phase plots like Fig. 5(b). By averaging over a number of samples of length 60, 120 and 240, bands we find $P_3 = 11.02 \pm 0.12P_1$, $P_3 = 11.06 \pm 0.07P_1$, $P_3 = 11.07 \pm 0.04P_1$ respectively, where the error is the standard deviation from the mean. The decrease in the standard deviation for the longer records shows that there is a long-term stability in P_3 underlying the short-term variations, and from these results we may conclude that P_3 varies by less than one part in 250, when averaged over long periods. Interstellar scintillation prevented a determination of P_3 over longer time scales, except for one period

spanning 350 bands. Fitting the subpulse-band phase for this period with lines of different slope we find $P_3 = 11.04 \pm 0.02P_1$. This result is not directly comparable with those above, which refer to averages of a number of records, but it is clear that the long term stability of P_3 , for this one period at least, agrees with the shorter term averages to within \sim one part in 500. If no allowance had been made for phase jumps at nulls a larger mean value of P_3 and much poorer stability would result, since the lengths and frequency of nulls then become directly relevant.

It is of interest to compare our observations of PSR 0809 + 74 with those of other pulsars showing drifting subpulses and published elsewhere (e.g. Taylor & Huguenin 1971; Huguenin, Taylor & Troland 1970; Taylor, Manchester & Huguenin 1975). We have found plots of a number of nulls in the literature, in which the phase behaviour is the same as that which we report here, and it is therefore surprising that the very simple relationship between null duration and phase has not been noticed before. We have not found any examples which were inconsistent with our interpretation. A good example of the cessation of pulse drifting during a null is shown by PSR 0031 – 07. This exhibits drifting subpulses in bursts of pulses, and the pulsar is in a nulled state for a much larger proportion of the time than PSR 0809 + 74 (Huguenin *et al.* 1970). Taylor *et al.* (1975) show a subpulse-band diagram for PSR 0031 – 07 with an unusually short null of length $L = 8$. The subpulse-band behaviour observed here is clearly consistent with the halt of drift during the nulled pulses.

4 Discussion

In PSR 0809 + 74 we have seen (Fig. 1) that the spacing of consecutive bands is very regular, and our observations show that P_2 is the most stable short-term subpulse parameter, in agreement with Taylor *et al.* (1975). In the present observation we find that the rms scatter in P_2 is less than 8 per cent. This high stability of P_2 persists even in the subpulse bands following a null, so we may conclude that the occurrence of a null does not noticeably affect the spacing of subpulse bands.

Relatively stable drifting of bands thus starts immediately the pulsar recommences radiating after a null, and this is important in view of the phase behaviour observed at nulls. We have seen in Section 3 that the first pulse after a null has a subpulse at the same position in the pulse window, and hence at the same phase, as that expected of the first nulled pulse. Since the step in phase of $\psi(N)$ following a null is found to persist indefinitely it is clear that all the emitting regions, giving rise to one subpulse band each, must experience a null (and cease drifting) simultaneously, because the spacing between subsequent bands would otherwise be altered – and, in our experience, this is never the case. Thus in PSR 0809 + 74 all the radiation in drifting subpulses must cease for the duration of a null, independent of the line of sight. The nulls cannot therefore be caused by deflection of the radiation from the line of sight to the Earth. In addition, for this particular pulsar, all the radiofrequency emission occurs in drifting subpulses, and we therefore conclude that *all* radio emission from PSR 0809 + 74 ceases during a null.

Our results therefore show that the nulling mechanism must be very closely linked with the process which causes the drift of subpulses. This has important implications for any model which attempts to explain the drifting subpulse phenomenon. As an example, we choose the model proposed by Ruderman & Sutherland (1975), hereafter referred to as RS. This is the most detailed model yet presented for the pulsar emission mechanism. It has been criticised on theoretical grounds by various authors (Hillebrandt & Müller 1976; Flowers *et al.* 1977), as a result of which the model has been revised (Cheng & Ruderman 1977). In this model the drifting subpulse phenomenon is explained by associating each subpulse

band with a spark of e^+e^- pairs which appears in the magnetospheric gap or the space-charge limited region above the magnetic polar cap. If the location of each spark is determined by the electrons flowing down to the surface of the pulsar, the sparks drift around the magnetic pole, and the beam of radiation due to each spark moves relative to the stellar surface, thus causing the subpulses to drift.

The regular spacing of successive subpulses shows that the sparks in the RS model must be equi-spaced around the magnetic pole. The phase behaviour observed at each null implies that all sparks must cease drifting and recommence drifting within a small fraction of the basic pulse period, P_1 , since if some sparks continued to drift while others were stationary with respect to the corotating frame, the regular pattern of subpulse bands would be broken up, and this is not observed. Moreover, since no *stationary* subpulse bands are ever observed in PSR 0809 + 74, it is clear that the radiation originating in each spark must also cease when the spark ceases to drift. Thus we may conclude that at a null both the radiation originating in all sparks and the drift of all sparks must cease.

The fact that the subpulse radiation recommences with the phase expected of the first nulled pulse shows that a form of memory must exist during nulls which ensures that pulsing begins at the correct phase after a null. This memory persists at least as long as the longest null observed ($10P_1$ in PSR 0809 + 74, and much longer in PSR 0031 – 07). However, the phase at which nulls occur has been found to be random, which implies that the memory does not affect the occurrence of nulls.

A possible explanation for the nulls is the temporary quenching of sparks. This would be consistent with the cessation of subpulse drifting during a null, because the drift of the pattern depends on the electrons travelling down to the pulsar surface. The observed phase behaviour then implies that *all* the sparks must be quenched during a null and that the memory must extend over the whole polar cap. When pulsing recommences the sparks must restart where they stopped, and immediately resume steady precession with a regular spacing between them. An order of magnitude estimate indicates that heating of the surface by electrons could give rise to a characteristic temperature distribution sufficiently long-lived to explain the memory effect.

The possibility that nulls are caused simply by the deflection of magnetic field lines can definitely be ruled out by the observed phase behaviour: the radiation would simply be deflected from the line of sight without affecting the phase of the subpulses following a null (in which case Fig. 7(a) would show the least phase disturbance coincident with a null).

No detailed model of the spark mechanism has been worked out in the RS model, but the simultaneous cessation and recommencement of drift of all sparks during and following nulls, the persistence of memory for the duration of nulls, and the equal spacing of the sparks are very stringent requirements for a simple sparking mechanism. The symmetry implied by the equi-spacing of the emitting regions could originate in a multipole magnetic field configuration, which might also be the basis of the memory during nulls, and of the high long-term stability of P_3 . At low frequencies, three subpulses may be seen in a single pulse, and therefore there are probably at least four of these emitting regions. Sparks may indeed be instrumental in producing drifting subpulses in such a scheme, but it is clear that sparks in the simple field configuration of the RS model, which are caused to drift simply by the departure from corotation at the polar cap, cannot be responsible for the observed behaviour in PSR 0809 + 74.

Acknowledgments

We thank Professor A. Hewish for stimulating discussions which initiated this work, and Dr R. D. Blandford for helpful comments on the text. ACSR gratefully acknowledges the sup-

port of the Royal Society Weir Research Fellowship and of a Visiting Research Fellowship at the California Institute of Technology. SCU acknowledges the support of an SRC studentship. This work was supported in part by NSF grant number MPS 73-04677.

References

- Backer, D. C., 1970. *Nature*, **227**, 692.
Cheng, A. F. & Ruderman, M. A., 1977. *Astrophys. J.*, **212**, 800.
Cole, T. W., 1970. *Nature*, **227**, 788.
Drake, F. D. & Craft, Jun., H. D., 1968. *Nature*, **220**, 231.
Flowers, E. G., Lee, J.-F., Ruderman, M. A., Sutherland, P. G., Hillebrandt, W. & Müller, E., 1977. *Astrophys. J.*, **215**, 291.
Hillebrandt, W. & Müller, E., 1976. *Astrophys. J.*, **207**, 589.
Huguenin, G. R., Taylor, J. H. & Troland, T. H., 1970. *Astrophys. J.*, **162**, 727.
Lyne, A. G., Smith, F. G. & Graham, D. A., 1971. *Mon. Not. R. astr. Soc.*, **153**, 337.
Page, C. G., 1973. *Mon. Not. R. astr. Soc.*, **163**, 29.
Ruderman, M. A. & Sutherland, P. G., 1975. *Astrophys. J.*, **196**, 51.
Taylor, J. H. & Huguenin, G. R., 1971. *Astrophys. J.*, **167**, 273.
Taylor, J. H., Manchester, R. N. & Huguenin, G. R., 1975. *Astrophys. J.*, **195**, 513.